



Article

Fatigue Life Analysis of Automotive Cast Iron Knuckle under Constant and Variable Amplitude Loading Conditions

Kazem Reza Kashyzadeh^{1,2,*}, Kambiz Souri³, Abdolhossein Gharehsheikh Bayat³, Reza Safavi Jabalbarez³ and Mahmood Ahmad^{4,5}

¹ Department of Transport, Academy of Engineering, Peoples' Friendship University of Russia (RUDN University), 6 Miklukho-Maklaya Street, 117198 Moscow, Russia

² Mechanical Characteristics Laboratory, Center for Laboratory Services, Sharif University of Technology, Tehran 11365, Iran

³ Department of Mechanical and Instrumental Engineering, Academy of Engineering, Peoples' Friendship University of Russia (RUDN University), 6 Miklukho-Maklaya Street, 117198 Moscow, Russia; suri-k@rudn.ru (K.S.), 1042175135@rudn.ru (A.G.B.), 1042188039@rudn.ru (R.S.J.)

⁴ Department of Civil Engineering, Faculty of Engineering, International Islamic University of Malaysia, Jalan Gombak 50728, Selangor, Malaysia; ahmadm@iiium.edu.my

⁵ Department of Civil Engineering, University of Engineering and Technology Peshawar, Bannu Campus, Bannu 28100, Pakistan

* Correspondence: kazem.kashyzadeh@gmail.com or reza-kashi-zade-ka@rudn.ru

Abstract: The main aim of the present paper is to assess the fatigue lifetime of ductile cast iron knuckles as one of the critical components of an automotive steering system. To this end, a real driving path, including various maneuvers, such as acceleration, braking, cornering, and moving on various types of road roughness, was considered. Different load histories, which are applied on various joints of the component (i.e., lower control arm, steering linkage, and Macpherson strut), were extracted through Multi-Body Dynamics (MBD) analysis of a full vehicle model. The achievements of previous studies have proved that the steering knuckle fails from the steering linkage and due to the rotational motion. Therefore, only this destructive load history was considered in future analyses of the present study. The CAD model was created using Coordinate Measuring Machine (CMM) data and some corrections in CATIA software. Furthermore, transient dynamic analysis was performed, and the time history of von Mises equivalent stress was obtained at the root of the steering linkage (which is exactly the location of failure based on the laboratory data as well as finite element simulations validated by the author in the previous studies). To predict the fatigue life of a component, two different methodologies were considered. Firstly, some well-known criteria were employed for equalization of load spectrum to a Constant Amplitude Loading (CAL). Then, fatigue analysis under sinusoidal loading was performed. Secondly, the fatigue life of the component considering Variable Amplitude Loading (VAL) was predicted using the Critical Plane Method (CPM), employing the Rain-flow cycle counting technique, and utilizing the Miner–Palmgren damage accumulation rule. Eventually, to evaluate the prediction accuracy of different methodologies, the obtained results were compared with the full-scale axial variable amplitude fatigue test which was performed by the corresponding author. The results indicated that the prediction of variable amplitude fatigue lifetime by Finite Element (FE) analysis in the time domain has about 21% error compared to reality. Additionally, the relative error between the results obtained from two different methodologies is about 20%, which is acceptable due to the scattering of the fatigue phenomenon results, the complex geometry of the part, and the complicated loading.

Keywords: steering knuckle; fatigue analysis; fatigue life; load spectrum; different maneuvers; finite element simulation



Citation: Reza Kashyzadeh, K.; Souri, K.; Gharehsheikh Bayat, A.; Safavi Jabalbarez, R.; Ahmad, M. Fatigue Life Analysis of Automotive Cast Iron Knuckle under Constant and Variable Amplitude Loading Conditions. *Appl. Mech.* **2022**, *3*, 517–532. <https://doi.org/10.3390/applmech3020030>

Received: 27 March 2022

Accepted: 22 April 2022

Published: 25 April 2022

Publisher's Note: MDPI stays neutral with regard to jurisdictional claims in published maps and institutional affiliations.



Copyright: © 2022 by the authors. Licensee MDPI, Basel, Switzerland. This article is an open access article distributed under the terms and conditions of the Creative Commons Attribution (CC BY) license (<https://creativecommons.org/licenses/by/4.0/>).

1. Introduction

Engineering structures, mechanical components, and assemblies commonly experience complicated cyclic loadings that eventually lead to fatigue failures [1–7]. In this regard, some published papers have reported that the fatigue phenomenon is the main cause of 50–90% of failures of in-service mechanical components [8–10]. Hence, it is important to assess the fatigue life of mechanical components in the design phase. In other words, selecting the proper geometries and material properties according to the details of the exerted axial, biaxial, or multiaxial loadings and the trends of variations of time histories of different applied loads is a vital task in the design stage. Loads of the engineering structures are usually random in nature, in which the stress components may change over time. This type of loading is known as Random Loading (RL), and the simplified case is that the time interval of these changes is constant, which is called the Variable Amplitude Loading (VAL). Therefore, analyzing structures and parts under real conditions (i.e., RL) is very difficult, time consuming, and costly. For this reason, many scientists have tried to simplify real loads with very good accuracy and perform simulations and estimates with acceptable accuracy and save time and money. In particular, these problems become more apparent when the subject is the destructive phenomenon of fatigue. Moreover, the number of load inputs and their combination, as well as the complexity of the geometry of the components have a significant impact on the difficulty presented above. In this study, the steering knuckle as one of the most critical mechanical parts of the passenger car was investigated in a case study, to which all of the above applies. All the road-induced vertical (ride), lateral (handling and steering), and longitudinal (braking or acceleration) forces are directly exerted on the knuckle of the passenger car and, thus, this component is subjected to the largest loads. Additionally, this component has a complex and variable geometry. In other words, its geometry changes depending on the specifications of the steering system and the suspension system, including the spatial coordinates of other parts, assembly constraints, and joints, etc. [11,12]. However, depending on the classification of the car, different materials (cast iron, forged iron, aluminum, and composite materials) are used to make the car steering knuckle [13].

In preliminary research, scientists have investigated the instantaneous strength of this supercritical component under static loading [14–18]. In most of this group of studies, the applied load is considered equal to the maximum value of the dynamic load on the component during different driving maneuvers. Additionally, higher strengths are achievable through detecting the weak regions of the components under different conditions and modifying the geometry to present an optimized design. The geometrical optimization of the knuckle based on static strength and deflection constraints has been accomplished by some scholars [19–24] to reduce the weight of the mentioned component by considering the reduction of fuel consumption and emissions. For example, Sharma et al. have conducted a static analysis of steering knuckle and shape optimization. The different loads, such as braking torque, longitudinal and vertical reaction, and steering reaction are applied to analyze it. In this research, aluminum alloy 2011-T3 is reported as the best material for designing the knuckle [17]. Tagade et al. have performed a static analysis of steering knuckles by assuming two types of materials. The FEM results (total deformation and shear stress in XY plane) are compared for both materials. Finally, shape optimization is utilized to reduce the mass of the knuckle by about 67% [22]. Vivekananda et al. have applied a metal matrix composite to reduce the weight of the knuckle. The critical location is determined by performing structural and fatigue analysis during different maneuvers. Finally, the knuckle's performance before and after optimization is compared through fatigue, impact analysis, and vibration test data [25]. Babu et al. have studied the stress analysis of knuckles under the actual load conditions as a time function [26]. Pingqing et al. have simulated the multi-body dynamics of the suspension system to obtain the bearing load under the actual working conditions. Then, strength analysis of the steering knuckle is performed based on these conditions [27].

Despite past research, numerous accidents have recently been reported due to the failure of steering components. For future studies and to find the cause of the failures, the fatigue life of the steering knuckle has been investigated [28–31] considering different driving conditions. The more remarkable studies have considered constant amplitude loadings and axial fatigue simulation by utilizing commercial finite element analysis codes. Sivananth et al. have carried out the fatigue and impact analysis of automotive steering knuckles under operating load cases. Additionally, the static analysis is performed for Spheroidal Graphite (SG) iron and Al alloy under different loadings. The results showed that the steering arm is a critical zone that is likely to fail. Then, the fatigue life is predicted using the S-N approach. The impact analysis has been conducted on the knuckle at different speeds of 2 and 4 m/s [32]. Triantafyllidis et al. have studied fatigue and fracture characteristics of a knuckle made of ductile iron. From the small broken part of the knuckle and near the fracture surface, a 10-mm-thick slice is cut off to perform chemical analysis by Optical Emission Spectroscopy (OES) and optical metallography. Then, the specimen is provided for the Charpy V-notch impact test. Scanning Electron Microscope (SEM) images have been used to do the topography analysis of the fracture surface. Finally, the fatigue phenomenon is proposed as the main reason for this failure [33].

In the past decades, the researchers have found that multiaxial rather than uniaxial fatigue life assessment procedures should be employed for the majority of mechanical and automotive components. The results of a comprehensive study have shown that the multi-axial fatigue life of the automotive steering knuckle is significantly less than the axial fatigue life of the component. Additionally, in a case study, the conversion ratio of these two types of analysis is reported in the range of 0.78 to 0.83 [34]. To overcome this issue, different criteria and various methodologies have been proposed [35–39]. However, most of these criteria give reasonable results for proportional loading but cannot be used to predict the general case of multiaxial fatigue life assessment under non-proportional, and especially random fluctuations of stress components. These researchers have mainly proceeded based on the assumption of a fixed critical plane; this assumption is specific and under controlled conditions [40,41]. Farrahi et al. have investigated fatigue damage to the rear spindle of the vehicle [42]. Fatemi et al. have studied the effect of various parameters of the production process on the fatigue life of a steering knuckle made of forged steel by using experimental [43] and analytical [44] methods. Zoroufi et al. have undertaken the experimental durability assessment and life prediction of steering knuckles made of different materials including forged steel, cast iron, and aluminum alloy [45]. Sonsino et al. have estimated the multiaxial fatigue life of automotive safety components made of cast aluminum under constant and variable amplitude loadings [46]. The fatigue life of a vehicle knuckle has been improved via a reliability-based design optimization approach [47]. The fatigue life and impact behavior of a steering knuckle made of titanium carbide and reinforced with metal matrix composites have been investigated to reduce the weight of the knuckle [11,32]. The fatigue life of a vehicle suspension system has been predicted for different types of materials (cast carbon steel, malleable cast iron, Ti-13V-11Cr-3Al, and Zinc AG40A cast) through FEM simulation [48]. In this respect, Kulkarni et al. have assessed the fatigue life of a suspension system for an in-wheel electric vehicle [49]. Similarly, Ossa et al. have predicted the fatigue life of a car suspension system ball joint [50]. Kashyzadeh et al. have assessed the service life of suspension packages of automobiles by random vibration fatigue analysis associated with road roughness [51]. Additionally, Chin et al. have studied the fatigue life of suspension lower arms through vibration fatigue analysis in the frequency domain [52].

Given the literature review, a summary of the reported results, and the above-mentioned issues, a brief description of the innovations of the present research is as follows:

1. Considering the equivalent road involves different maneuvers and various speeds;
2. Driving simulation of a full vehicle model (taking into account the masses, inertia, and actual characteristics of the car) on the real road in the MBD software (Adams/Car, MSC Software Company, Irvine, CA, USA);

3. Extracting the time histories of loads applied to the steering knuckle connections in different directions as a result of crossing a real road;
4. Use of different methodologies to convert VAL to CAL based on the assumption of the same fatigue damage;
5. Assessing the fatigue life of cast iron steering knuckle in both constant and variable amplitude loading based on the real road conditions and a combination of actual maneuvers, and finally, compared with full-scale laboratory results.

2. Material

In the present research, the front left side steering knuckle made of ductile cast iron of a passenger car was studied (Figure 1). From this figure, the steering knuckle is connected to the MacPherson suspension system and steering system linkage. Additionally, this component is responsible for carrying the wheel spindle and parking system. For this reason, this component is known as a supercritical component in the automotive and by failing, it can affect any of the above systems and take the control of the vehicle away from the driver and ultimately lead to accidents (and sometimes irreparable damage, such as driver and passenger deaths). To accurately identify the material and its mechanical properties, standard specimens for various tests, including quantometric, metallographic, tensile testing, and fatigue testing, were fabricated from different parts of this component as shown in Figure 2. The chemical composition (wt%) of the considered material is presented in Table 1 [53]. Moreover, the mechanical properties of the material are given in Table 2 [53]. Additionally, the cyclic characteristics of ASTM A536-Grade 65-45-12 were assumed as in the previous paper [54] (Table 3).

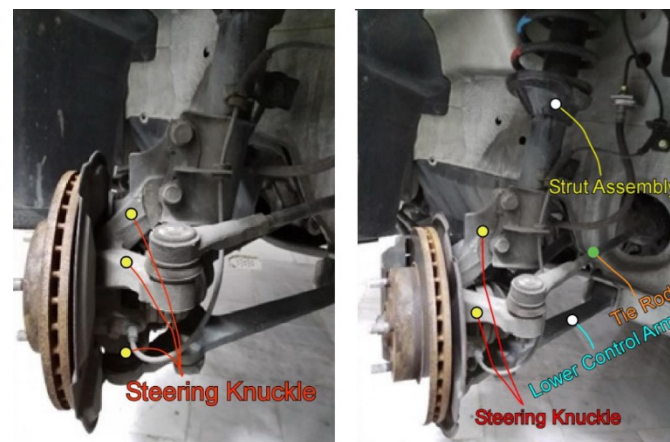


Figure 1. The considered automotive cast iron knuckle [53,55].

Table 1. Chemical composition (wt%) of the cast iron steering knuckle [53].

Fe	Base	C	3.63	Si	2.77	Mn	0.144
----	------	---	------	----	------	----	-------

Table 2. Mechanical properties of ductile cast iron [53].

Tensile Strength	Yield Strength	Poisson's Ratio	Elastic Modulus	Density
(MPa)	(MPa)		(GPa)	(g/cm ³)
480	328	0.28	144.7	7.1

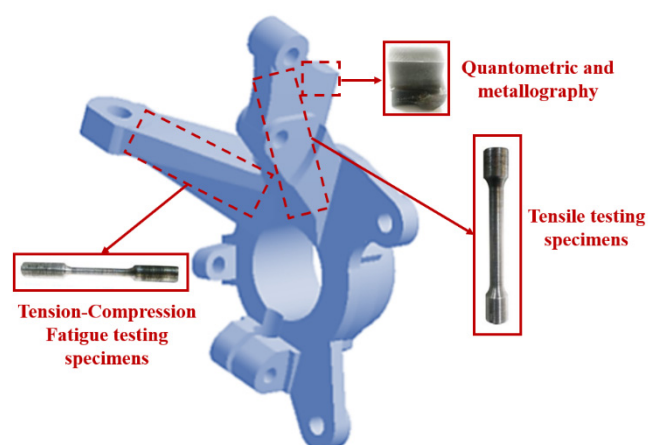


Figure 2. Fabrication of different standard samples from automotive steering knuckles for performing various material, metallurgy, and mechanical experiments.

Table 3. Cyclic characteristics of ASTM A536-Grade 65-45-12 [54].

	Properties	Symbol	Value	Unit
Strain-Life Morrow Life SWT Life	Fatigue strength coefficient	\acute{S}_f	585	MPa
	Fatigue strength exponent	b	−0.075	—
	Fatigue ductility coefficient	\acute{E}_f	0.666	—
	Fatigue ductility exponent	c	−0.751	—
Cyclic Stress-Strain	Cyclic strain hardening exponent	\acute{n}	0.14	—
	Cyclic strength coefficient	\acute{k}	877	—
	Cyclic modulus of elasticity	\acute{E}	1.447×10^5	MPa
S-N data	Extend of the First slope line to the vertical axis of the S-N curve	SRI 1	1111	MPa
	The first slope of the logarithmic S-N curve	b_1	−0.075	—
	The second slope of the logarithmic S-N curve	b_2	0	—

3. MBD Analysis of Full Vehicle Model

A combination of different types of maneuvers was considered for the equivalent road simulation in Adams/Car software as follows [56]:

$$R_{eq} = \left(\alpha_{\text{straight}} + \alpha_{\text{braking}} + \alpha_{\text{acceleration}} + \alpha_{\text{cornering}} \right) \times X \quad (1)$$

where:

X is the road length, R_{eq} and α_i are the equivalent road and the share of various ISO road classifications in percentage, respectively. Moreover, braking and acceleration maneuvers were neglected in the present study. Because the results presented in previous research have proved that their impacts on fatigue damage of auto parts are not significant compared to the influence of straight driving [56,57]. Finally, the details of the equivalent road consist of 95% straight driving and 5% fast cornering effects are depicted in Figure 3.

Next, the driving a four-cylinder passenger car with 1670 kg gross weight including several main sub-models, such as the MacPherson front suspension system, twist beam for the rear suspension system, rack and pinion types of steering systems, front and rear wheels, body, etc., was simulated [58,59]. The distance between two lateral axes and between the rear and front axles are 1455 and 2415 mm, respectively. The values of suspension system parameters are presented in Table 4. The tires were modeled as 175/70/R13 for the present research. Moreover, based on the settings of the car manufacturer, the Toe and Camber

angles were considered as -0.1 and $+2$ degrees, respectively [56]. Figure 4 illustrates the full vehicle model in Adams/Car software based on reality.

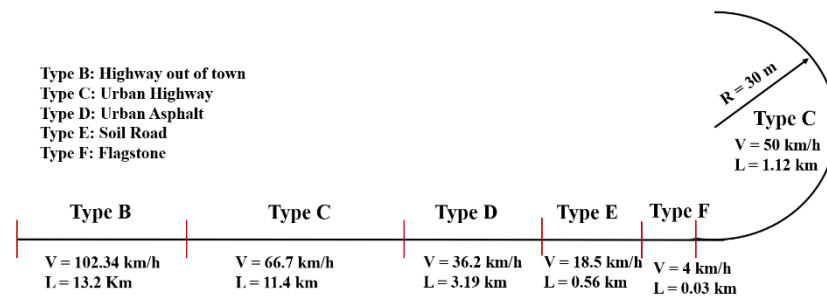


Figure 3. The details of equivalent road used in the MBD analysis.

Table 4. Values of suspension system parameters.

Parameter	Unit	Value
Front suspension stiffness	N/m	35,000
Rear suspension stiffness	N/m	38,000
Damping coefficient of suspension in traction mode (both front and rear)	N·s/m	1000
Damping coefficient of suspension in compression mode (both front and rear)	N·s/m	720
Tires spring stiffness	N/m	190,000
Damping coefficient of tires	N·s/m	10

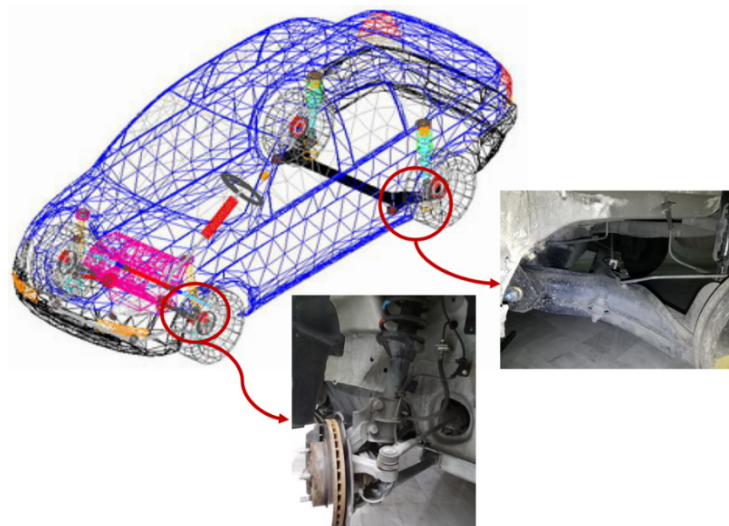


Figure 4. Full vehicle model in Adams/Car Software based on reality [56].

At the last stage of the MBD simulation of the car moving on the equivalent road, the time histories of the forces applied to the different joints of the steering knuckle were extracted in various directions (X, Y, and Z). Eventually, the various steps in this part of the research are summarized in detail in Figure 5 as a practical algorithm. However, only the force history in the Z direction applied to the steering linkage was considered the most destructive factor of failure [34,55] (Figure 6).

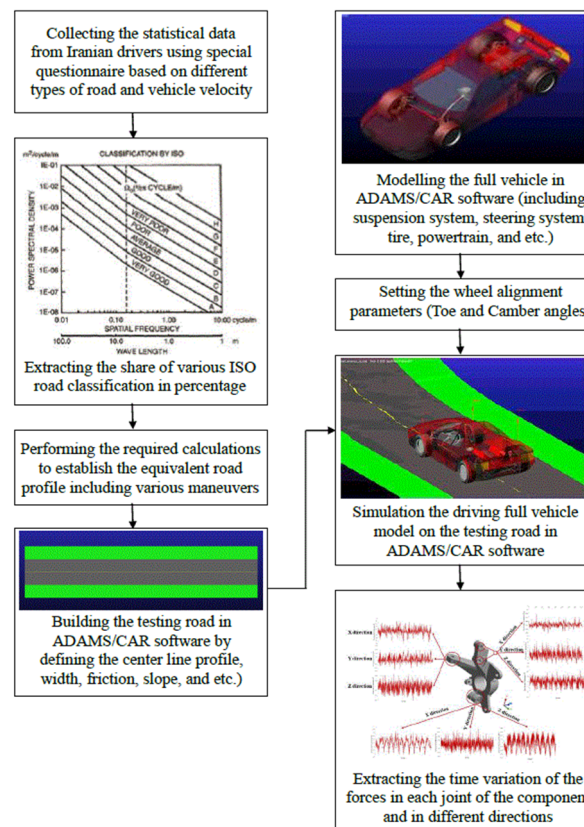


Figure 5. The practical algorithm of force-time histories extraction process based on the multi-body dynamics simulation [55,56].

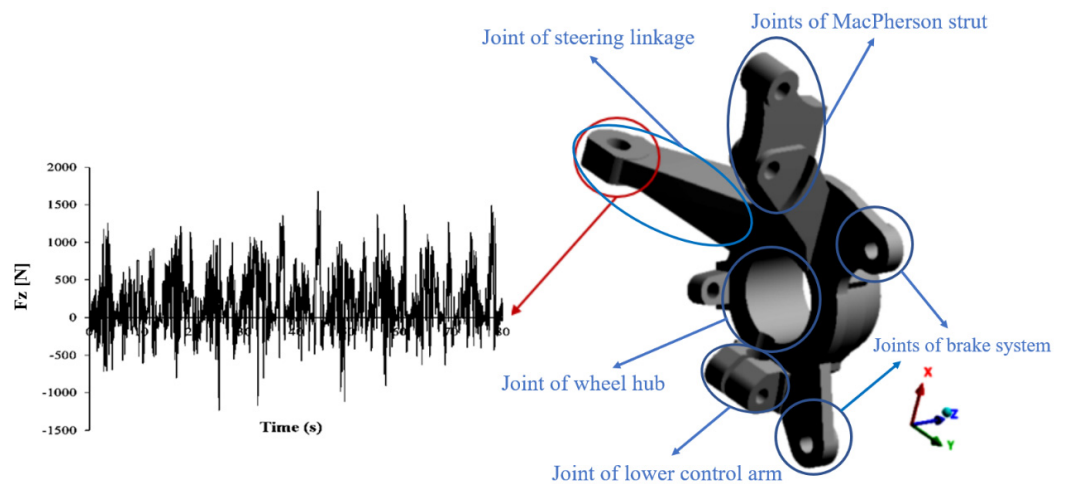


Figure 6. The details of loading history, its location, and the applied direction in the present research.

4. Finite Element Model

The primary model of the steering knuckle geometry was prepared using CMM data and employing the cloud points module in CATIA modeling software. Thus, the most accurate geometric model (close to reality), including complete details, such as serial numbers, production data, and surface defects, was created [13]. However, previous research has suggested that such a model is not suitable for finite element analysis (in some places, such as serial number indentations, it is not possible to mesh accurately). To overcome this problem, it is necessary to modify some of the above-mentioned details

and create a smooth model [13]. Figure 7 demonstrates a corrected version of the steering knuckle geometry (smooth model).



Figure 7. A corrected version of the steering knuckle geometry (smooth model) [13].

Solid elements with different grid sizes were used for meshing homogeneously with equal grid sizes. After that, the mesh convergence study was performed to select the minimum number of meshes with the highest response accuracy. In other words, it was conducted to reduce computational costs because fatigue analysis is very complex and time consuming. Eventually, the FEM used for future analysis in this study is shown in Figure 8, which has 51,858 elements [53].

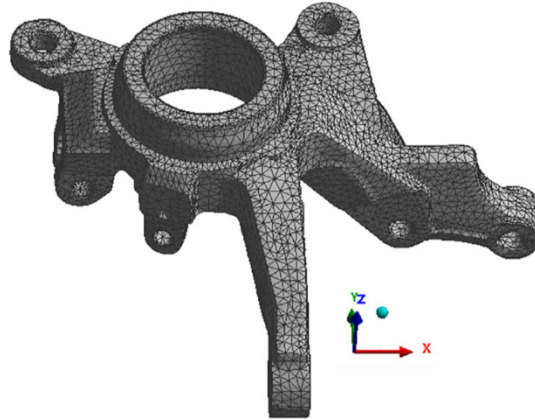


Figure 8. The FEM of the automotive steering knuckle based on sensitivity analysis of response to the number of meshes [53].

Next, the material was assigned to the finite element model as described in Section 2. Additionally, the loading history extracted from the results of MBD analysis was applied to the connection hole of the steering knuckle to the steering linkage. The wheel hub was fixed in all degrees of freedom (DOF).

5. Fatigue Life Prediction

5.1. Using Some Well-Known Criteria for Equalization of Load Spectrum to a CAL

In general, the conversion of a VAL to a CAL is based on the principle of the same fatigue damage in both loads. However, the effects of the precedence and latency of peaks and valleys on loadings cannot be modeled. Therefore, there are differences between different criteria in calculating fatigue life. In the study of the fatigue phenomenon in the

high cycle regime, the Basquin equation uses the simplest and one of the most common relationships as follows:

$$N = k \times S_r^{-m} \tag{2}$$

In which, N represents the number of cycles to failure, S_r is alternative stress, and k and m are the material coefficients, which are obtained from the laboratory tests or S-N diagram. Hence, the fatigue damage for a load spectrum consisting of n cycles with alternative stresses of S_{r_i} is:

$$D = \sum_{i=1}^n \frac{1}{k \times S_{r_i}^{-m}} \tag{3}$$

Assuming the same fatigue damage in two spectra:

$$\frac{N_{eq}}{k \times S_{req}^{-m}} = \sum_{i=1}^n \frac{1}{k \times S_{r_i}^{-m}} \tag{4}$$

As a result, the equivalent fatigue life is obtained as follows:

$$N_{eq} = \sum_{i=1}^n \left(\frac{S_{req}}{S_{r_i}} \right)^{-m} \tag{5}$$

The above equation is true for a completely inverse loading ($R = -1$). However, in a VAL, the average load is usually not zero. Therefore, it is necessary to combine this equation with the criteria that include the effect of mean stress. The following is a brief description of the most well-known ones that have been used in this study.

5.1.1. Goodman Criterion

The general relationship proposed to consider the effect of mean stress is as follows:

$$\frac{S_r}{\hat{S}_r} + \frac{S_m}{S_u} = 1 \tag{6}$$

where \hat{S}_r is equivalent stress considering $R = -1$, and S_m and S_u are the mean stress and ultimate strength, respectively. By combining this equation with Equation (5), we have [60]:

$$N_{eq} = \sum_{i=1}^n \left(\frac{S_{req}}{S_{r_i}} \times \frac{S_u - |S_{m_i}|}{S_u - |S_{m_{eq}}|} \right)^{-m} \tag{7}$$

5.1.2. Soderberg Criterion

The general relationship is proposed to consider the effect of mean stress is as follows:

$$\frac{S_r}{\hat{S}_r} + \frac{S_m}{S_y} = 1 \tag{8}$$

In fact, the main difference between Soderberg and Goodman criteria is the use of yield stress (S_y) instead of ultimate stress (S_u). Therefore, the equivalent fatigue life is calculated as [60]:

$$N_{eq} = \sum_{i=1}^n \left(\frac{S_{req}}{S_{r_i}} \times \frac{S_y - |S_{m_i}|}{S_y - |S_{m_{eq}}|} \right)^{-m} \tag{9}$$

5.1.3. Gerber Criterion

In this criterion, the following relation is presented to consider the effects of mean stress on the fatigue behavior of the metal material.

$$\frac{S_r}{\hat{S}_r} + \left(\frac{S_m}{S_u} \right)^2 = 1 \tag{10}$$

Finally, by substituting Equation (10) into the Equation (5) [60]:

$$N_{\text{eq}} = \sum_{i=1}^n \left(\frac{S_{\text{req}}}{S_{r_i}} \times \frac{S_u^2 - S_{m_i}^2}{S_u^2 - S_{m_{\text{eq}}}^2} \right)^{-m} \quad (11)$$

5.2. Fatigue Analysis Considering Actual Loading Conditions

First, stress analysis was performed in the time domain to determine the most critical region of the steering knuckle which is apt to fail under cyclic loading (for more information, refer to the previous paper published by the corresponding author (i.e., Figure 16 in [53]). Afterward, time histories of stress tensor components were extracted in the critical element. Next, the von Mises equivalent stress was obtained on 36 planes separated by 5° angle increments. The fatigue life was calculated on all planes using the Rainflow cycle counting method and employing the Miner–Palmgren damage accumulation rule. Finally, the minimum lifetime on those 36 planes was reported as the fatigue life of the cast iron steering knuckle subjected to different maneuvers.

6. Results and Discussion

The results of the stress analysis showed that the critical area detected by the present finite element model is consistent with the fracture zone under the full-scale axial fatigue test with variable amplitude loading (Figure 9). Moreover, this area has been reported as the prone zone to fatigue failure in the automotive steering knuckle by other scholars [12,28,32,33]. However, some researchers also reported another area as a failure zone [43–45,61]. They believed that the joint of the knuckle and MacPherson strut is critical and fails under cyclic loading faster than other areas. This is not in conflict with the results of this study. As stated in the literature review, this supercritical component does not have a definite geometry and is different depending on the design parameters for each type of automotive. In other words, the geometric features and even the loading conditions are not the same in all studies, and this issue makes the study of this component have certain complexities and the results do not overlap. In addition, the loading conditions subjected to this component also depend on the specifications of the vehicle, road quality [62], and driver behavior in various maneuvers [63]. In the present research, an Iran national automotive was used. Additionally, to extract real loads, contrary to routine research based on the Belgian roads [53], real conditions including Iranian roads as well as the behavior of local drivers were considered. However, the Belgian road conditions for this vehicle and special component had already been considered by the corresponding author and he again reported the same area as the failure region [53].

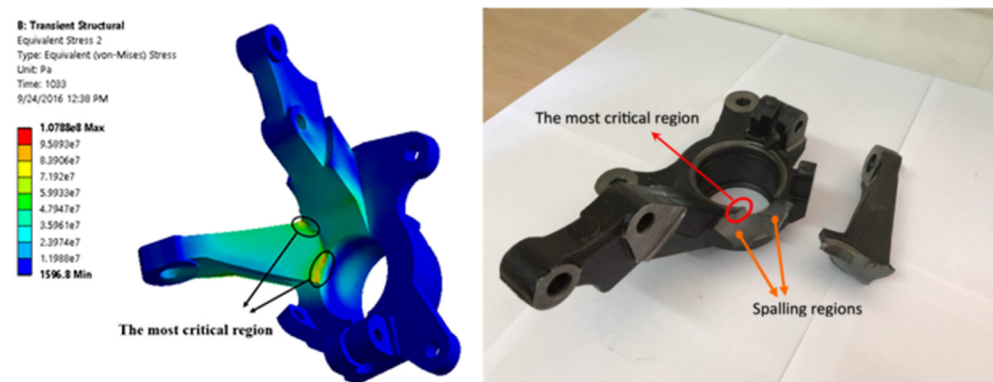


Figure 9. Comparison of fracture location in an experiment with area detection by FEM presented in this study [55].

The time histories of the stress tensor components ($\sigma_{ij}(t) = \begin{bmatrix} \sigma_{xx}(t) & \sigma_{xy}(t) & \sigma_{xz}(t) \\ \sigma_{yx}(t) & \sigma_{yy}(t) & \sigma_{yz}(t) \\ \sigma_{zx}(t) & \sigma_{zy}(t) & \sigma_{zz}(t) \end{bmatrix}$,

where $\sigma_{xy}(t) = \sigma_{yx}(t)$, $\sigma_{xz}(t) = \sigma_{zx}(t)$, and $\sigma_{yz}(t) = \sigma_{zy}(t)$) were extracted for all 36 planes in the critical region. Afterward, the von Mises criterion was used to calculate the equivalent stress history in all planes. However, there are various equivalent stress criteria, such as Findley [64], McDiarmid [64], modified Findley [65,66], modified McDiarmid [67], Dang Van [64], Carpinteri–Spagnoli [68], Liu–Zenner [65–67], Carpinteri [69], which are much more accurate than the von Mises criterion for variable amplitude loading. However, given the fact that their calculations are complex and time-consuming, the authors decided to use the von Mises criterion to reduce computational costs. Another advantage of this criterion compared to the rest is its availability in all finite element software and there is no need to use special coding or obtain coefficients through testing. Recently, various energy-based criteria have been proposed to estimate the fatigue life of components [70–72], which are more accurate than the above-mentioned criteria, but it should be noted that the complexity of these criteria is far greater than the critical plane-based criteria and cannot be found in commercial codes. Accordingly, in future studies, the authors try to use a combination of these criteria to evaluate this supercritical component more accurately.

A stress-time diagram of one plane, as a representative result, is shown in Figure 10. Additionally, the contours of the minimum fatigue life and the maximum fatigue damage of the component are illustrated in Figure 11a,b, respectively.

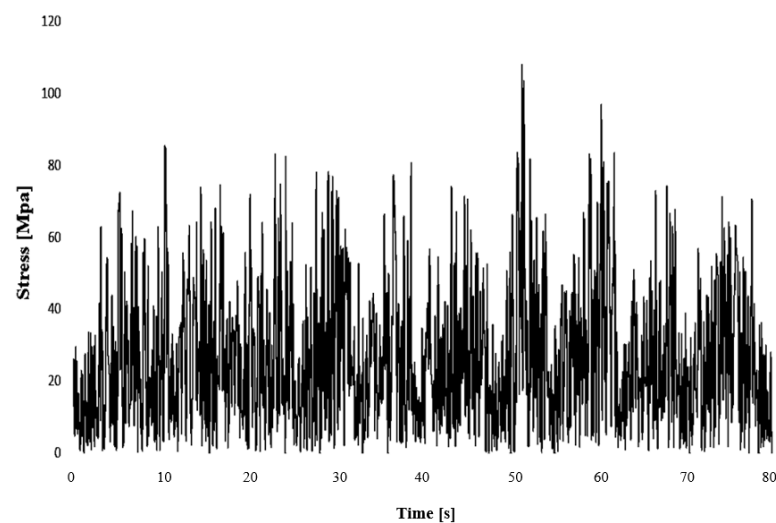


Figure 10. The von Mises equivalent stress-time diagram of one plane in the critical region, as a representative result.

Eventually, to verify the accuracy of the life prediction based on the different methodologies (CAL-based criteria and VAL as the actual loading) in this research, the obtained results were compared with the full-scale fatigue test result under axial variable amplitude loading (the corresponding author repeated this experiment for four cast iron steering knuckles of a passenger car and the mean value is reported as 423,758 times of repeat load block). Table 5 presents a summary of the results obtained in this research. Additionally, the error percentage of life assessment was calculated by applying the following formula [55].

$$\% \text{ Error} = \left| \frac{\text{fatigue life}_{\text{predicted}} - \text{fatigue life}_{\text{tested}}}{\text{fatigue life}_{\text{tested}}} \right| \times 100 \quad (12)$$

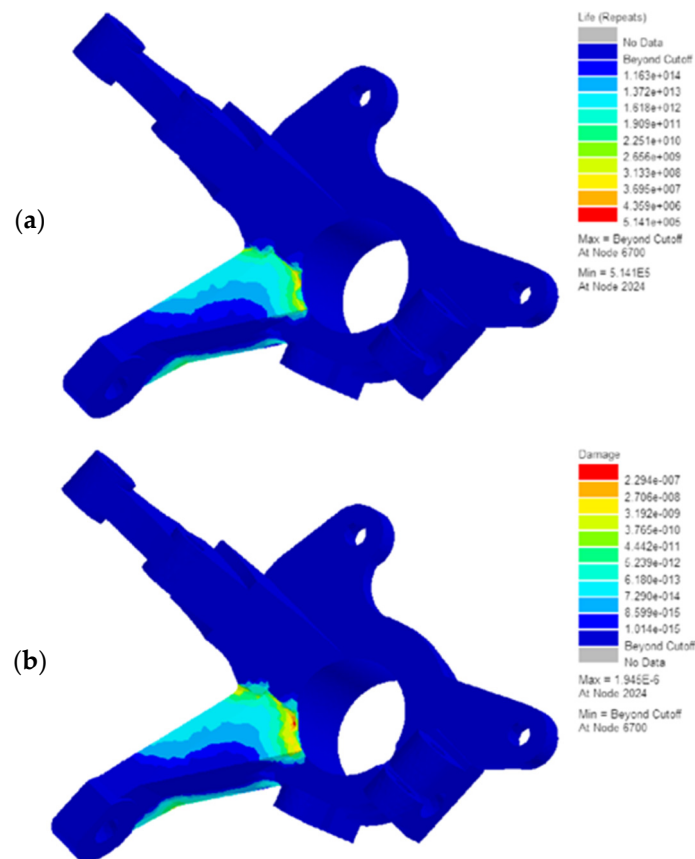


Figure 11. The results of fatigue analysis considering actual loading conditions, including (a) axial fatigue life contour of cast iron steering knuckle subjected to the different maneuvers and (b) fatigue damage contour of cast iron steering knuckle under axial variable amplitude loading caused by different maneuvers.

Table 5. Comparison of fatigue life prediction by utilizing different methodologies and experiment results.

Methodology	Criteria	Life Prediction (Cycle)	Error (%)
CAL	Goodman	661,825	56.18
	Soderberg	638,773	50.74
	Gerber	594,108	40.20
VAL	Actual loading in time domain (Von Misses equivalent stress history)	514,100	21.32

From Table 5, the prediction of axial fatigue life under variable amplitude loading is much closer to reality compared to the prediction of axial fatigue life under constant amplitude loading associated with different criteria. Taheri and Barati in their research on two widely used materials in the aerospace industry, including aluminum 7075-T6 and steel 4130, showed that using the relationships expressed in this research to equate variable amplitude loading with constant amplitude loading sometimes leads to large errors in fatigue results (this error is not negligible) [60]. They stated that if the loading is fully reversed, it can be equated with a very low error rate close to zero, but with increasing mean stress, this error increases (e.g., they reported an error rate of up to 80% for using the Goodman equation considering the load ratio of 0.4). Moreover, in this case study and according to the working conditions considered in this research, the Gerber criterion is

more suitable for converting VAL to CAL. Additionally, the results show that using the load conversion method creates a large error in estimating the fatigue life of automotive steering knuckles made of cast iron. However, papers published in this field, especially steering knuckles with complex geometry and multi-inputs random loading, sometimes have up to 50% error compared to reality. Therefore, to initially estimate the fatigue life of special parts with complex functions, it is appropriate to use this simplification. On the other hand, this is an error relative to reality, but compared to the more accurate method (i.e., VAL), this simplification increases the computational error by about 20%, which is cost-effective compared to how long it takes to solve the problem.

7. Conclusions

In the present research, the fatigue life of the automotive steering knuckle (a critical component with a complicated geometry) was predicted using FEM. Firstly, a multi-body dynamics analysis of a full vehicle model was conducted to extract load histories that are inserted into the connection points of the steering knuckle. In this regard, a real road was considered including various maneuvers and different road classifications based on the ISO standard. Additionally, the driving speed of the car on the road was simulated as a variable. Eventually, the history of destructive load in the automotive steering knuckle (the cause of fatigue) was determined in accordance with previously published papers. Next, two different methodologies were considered to estimate the fatigue life of this mechanical part. Firstly, simplification of loading history and conversion of variable amplitude to constant amplitude condition. Secondly, fatigue analysis in the time domain by applying VAL as the actual conditions. Finally, the results were compared with laboratory data to obtain the error value related to the use of these simplifications. Therefore, the following practical conclusions may be drawn from this comparison:

1. The results of the stress analysis showed that the critical area detected by the present finite element model is consistent with the fracture zone under the axial fatigue test with variable amplitude loading. On the other hand, the finite element model presented in this study can identify the fracture region in industrial components with complex geometries and tough loading conditions.
2. According to the findings of the present research, the prediction of variable amplitude fatigue lifetime by FE analysis in the time domain has about a 21% difference compared to reality. Additionally, the obtained results are acceptable due to the data scattering in this phenomenon and the complex geometry of the component. However, the von Mises equivalent stress is not accurate for non-proportional loading conditions.
3. The methodology of simplifying the loading history and converting the VAL to CAL by using different criteria to check the effects of mean stress in the calculations showed that 40–55% error is created compared to reality. However, due to the time consuming nature of other methodologies, this load conversion methodology can be used for the primary studies.
4. The results showed that for this case study, the best criteria for converting VAL to CAL with the aim of estimating fatigue life are Gerber, Soderberg, and Goodman criteria, respectively with approximately 40, 51, and 56% error relative to reality.
5. The results of this study indicated that the relative error between the results obtained from two different methodologies is 20%, and compared to the reduction in computational costs, this error is negligible (in the initial research phase).

Author Contributions: Conceptualization, K.R.K.; methodology, K.R.K.; software, K.R.K., K.S., A.G.B., R.S.J. and M.A.; validation, K.R.K.; formal analysis, K.R.K.; investigation, K.R.K., K.S., A.G.B., R.S.J. and M.A.; resources, K.R.K.; data curation, K.R.K.; writing—original draft preparation, K.R.K., K.S., A.G.B., R.S.J. and M.A.; writing—review and editing, K.R.K.; visualization, K.R.K.; supervision, K.R.K.; project administration, K.R.K.; funding acquisition, K.R.K. All authors have read and agreed to the published version of the manuscript.

Funding: This research received no external funding.

Institutional Review Board Statement: Not applicable.

Informed Consent Statement: Informed consent was obtained from all subjects involved in the study.

Data Availability Statement: The data that support the findings of this study are available from the corresponding author upon reasonable request.

Acknowledgments: This research has been conducted personally by the research team headed by Kazem Reza Kashyzadeh. Moreover, this paper has been supported by the RUDN University Strategic Academic Leadership Program.

Conflicts of Interest: The authors declare no conflict of interest.

References

- Rama Krishna, L.; Madhavi, Y.; Sahithi, T.; Srinivasa Rao, D.; Ijeri, V.S.; Prakash, O.; Gaydos, S.P. Enhancing the high cycle fatigue life of high strength aluminum alloys for aerospace applications. *Fatigue Fract. Eng. Mater. Struct.* **2019**, *42*, 698–709. [CrossRef]
- Vijayanandh, R.; Kumar, K.N.; Kumar, G.R.; Sanjeev, B.; Balachander, H.; Prasad, S.G. Comparative approaches for fatigue life estimation of aluminium alloy for aerospace applications. *Int. J. Veh. Struct. Syst.* **2018**, *10*, 282–286. [CrossRef]
- Abdollahnia, H.; Alizadeh Elizei, M.H.; Reza Kashyzadeh, K. Multiaxial Fatigue Life Assessment of Integral Concrete Bridge with a Real-Scale and Complicated Geometry Due to the Simultaneous Effects of Temperature Variations and Sea Waves Clash. *J. Mar. Sci. Eng.* **2021**, *9*, 1433. [CrossRef]
- Petrini, F.; Bontempi, F. Estimation of fatigue life for long span suspension bridge hangers under wind action and train transit. *Struct. Infrastruct. Eng.* **2011**, *7*, 491–507. [CrossRef]
- Abdollahnia, H.; Alizadeh Elizei, M.H.; Reza Kashyzadeh, K. Fatigue life assessment of integral concrete bridges with H cross-section steel piles mounted in water. *J. Fail. Anal. Prev.* **2020**, *20*, 1661–1672. [CrossRef]
- Ktari, A.; Haddar, N.; Rezai-Aria, F.; Ayedi, H.F. On the assessment of train crankshafts fatigue life based on LCF tests and 2D-FE evaluation of J-integral. *Eng. Fail. Anal.* **2016**, *66*, 354–364. [CrossRef]
- Amiri, N.; Shaterabadi, M.; Reza Kashyzadeh, K.; Chizari, M. A Comprehensive Review on Design, Monitoring, and Failure in Fixed Offshore Platforms. *J. Mar. Sci. Eng.* **2021**, *9*, 1349. [CrossRef]
- Kashyzadeh, K.R.; Arghavan, A. Study of the effect of different industrial coating with microscale thickness on the CK45 steel by experimental and finite element methods. *Strength Mater.* **2013**, *45*, 748–757. [CrossRef]
- Lee, Y.L.; Pan, J.; Hathaway, R.; Barkey, M. *Fatigue Testing and Analysis: Theory and Practice*; Butterworth-Heinemann: Oxford, UK, 2005; Volume 13, ISBN 0-7506-7719-8.
- Arghavan, A.; Reza Kashyzadeh, K.; Asfarjani, A.A. Investigating effect of industrial coatings on fatigue damage. In *Applied Mechanics and Materials*; Trans Tech Publications Ltd.: Bäch, Switzerland, 2011; Volume 87, pp. 230–237. [CrossRef]
- Vijayarangan, S.; Rajamanickam, N.; Sivananth, V. Evaluation of metal matrix composite to replace spheroidal graphite iron for a critical component, steering knuckle. *Mater. Des.* **2013**, *43*, 532–541. [CrossRef]
- Sivananth, V.; Vijayarangan, S. Fatigue Life analysis and optimization of a passenger car steering knuckle under operating conditions. *Int. J. Automot. Mech. Eng.* **2015**, *11*, 2417–2429. [CrossRef]
- Reza Kashyzadeh, K.; Farrahi, G.H.; Shariyat, M.; Ahmadian, M.T. Experimental and finite element studies on free vibration of automotive steering knuckle. *Int. J. Eng.* **2017**, *30*, 1776–1783. [CrossRef]
- Dumbre, P.; Mishra, A.K.; Aher, V.S.; Kulkarni, S.S. Structural analysis of steering knuckle for weight reduction. *Int. J. Emerg. Technol. Adv. Eng.* **2014**, *4*, 552–557.
- Madhusudhanan, S.; Rajendran, I.; Prabu, K. Static analysis of automotive steering knuckle. In *Applied Mechanics and Materials*; Trans Tech Publications Ltd.: Bäch, Switzerland, 2014; Volume 592, pp. 1155–1159. [CrossRef]
- Dusane, S.V.; Dipke, M.K.; Kumbhalkar, M.A. Analysis of steering knuckle of all terrain vehicles (ATV) using finite element analysis. In *IOP Conference Series: Materials Science and Engineering*; IOP Publishing: Bristol, UK, 2016; Volume 149, p. 12133.
- Sharma, M.P.; Denish, S.M.; Joshi, H.; Patel, D.A. Static analysis of steering knuckle and its shape optimization. *J. Mech. Civ. Eng.* **2014**, *4*, 34–38.
- Kadam, S.R.; Kale, P.D. Finite Element Analysis and Optimization of Automotive Steering Knuckle. *J. Interdiscip. Cycle Res.* **2020**, *12*, 115–119.
- Tang, G.; Shi, B.; Zhang, W. Structural response surface optimization design of steering knuckle arms under multiple working conditions based on fuzzy evaluation. *J. Eng. Sci.* **2013**, *35*, 1368–1374. [CrossRef]
- Lee, Y.C.; Jeon, N.J.; Kim, C.; Ahn, S.Y.; Cho, M.J. Shape optimization of a small bus steering knuckle considering a fatigue load. In *Advanced Materials Research*; Trans Tech Publications Ltd.: Bäch, Switzerland, 2013; Volume 740, pp. 319–322. [CrossRef]
- Teja, G.P.C.; Chandu, K.V.P.P.; Krishna, C.R.; Sreeram, K.Y. Weight optimization of steering knuckle joint using FEA. *Int. Res. J. Eng. Technol. IRJET* **2016**, *3*. Available online: <https://www.irjet.net/archives/V3/i12/IRJET-V3I12107.pdf> (accessed on 26 March 2022).
- Tagade, P.P.; Sahu, A.R.; Kutarmare, H.C. Optimization and finite element analysis of steering knuckle. *Int. J. Comput. Appl.* **2015**, *975*, 8887.

23. Borns, R.; Whitacre, D. *Optimizing Designs of Aluminum Suspension Components Using an Integrated Approach* (No. 2005-01-1387); SAE Technical Paper; SAE International: Warrendale, PA, USA, 2005. [[CrossRef](#)]
24. Shelar, M.L.; Khairnar, H.P. Design Analysis and Optimization of Steering Knuckle Using Numerical Methods and Design of Experiments. 2014. Available online: www.ijedr.org/papers/IJEDR1403012.pdf (accessed on 26 March 2022).
25. Vivekananda, R.; Mythra Varun, A.V. Finite element analysis and optimization of the design of steering knuckle. *Int. J. Eng. Res.* **2016**, *4*, 121–135.
26. Babu, B.; Prabhu, M.; Dharmaraj, P.; Sampath, R. Stress analysis on steering knuckle of the automobile steering system. *Int. J. Res. Eng. Technol.* **2014**, *3*, 363–366.
27. Pingqing, F.; Bo, Z.; Long, Q. The analysis on destruction forms of steering knuckle. In Proceedings of the 2011 Third International Conference on Measuring Technology and Mechatronics Automation, Shanghai, China, 6–7 January 2011; IEEE 2011; Volume 3, pp. 677–679. [[CrossRef](#)]
28. Madhusudhanan, S.; Kumar, K.A.; Kumar, V.P.; Mahendran, T. Fatigue analysis of automotive steering knuckle. *Mech. Mech. Eng.* **2016**, *20*, 5–13.
29. Kamal, M.; Rahman, M.M.; Rahman, A.G.A. Fatigue life evaluation of suspension knuckle using multi body simulation technique. *J. Mech. Eng. Sci.* **2012**, *3*, 291–300. [[CrossRef](#)]
30. Azrulhisham, E.; Asri, Y.M.; Dzuraidah, A.W.; Nik Abdullah, N.M.; Che Hassan, C.H.; Shahrom, A. Equilibrium Application of Road Simulator Service Loads in Automotive Component Durability Assessment. *Open Ind. Manuf. Eng. J.* **2011**, *4*, 1–7.
31. Niu, X.Y.; Wang, G.X.; Li, W. Finite element analysis of the car steering knuckle based on ANSYS. In *Applied Mechanics and Materials*; Trans Tech Publications Ltd.: Bäch, Switzerland, 2015; Volume 740, pp. 108–111. [[CrossRef](#)]
32. Sivananth, V.; Vijayarangan, S.; Rajamanickam, N. Evaluation of fatigue and impact behavior of titanium carbide reinforced metal matrix composites. *Mater. Sci. Eng. A* **2014**, *597*, 304–313. [[CrossRef](#)]
33. Triantafyllidis, G.K.; Antonopoulos, A.; Spiliotis, A.; Fedonos, S.; Repanis, D. Fracture characteristics of fatigue failure of a vehicle's ductile iron steering knuckle. *J. Fail. Anal. Prev.* **2009**, *9*, 323–328. [[CrossRef](#)]
34. Reza Kashyzadeh, K. Effects of axial and multiaxial variable amplitude loading conditions on the fatigue life assessment of automotive steering knuckle. *J. Fail. Anal. Prev.* **2020**, *20*, 455–463. [[CrossRef](#)]
35. Fatemi, A.; Socie, D.F. A critical plane approach to multiaxial fatigue damage including out-of-phase loading. *Fatigue Fract. Eng. Mater. Struct.* **1988**, *11*, 149–165. [[CrossRef](#)]
36. Socie, D. *Critical Plane Approaches for Multiaxial Fatigue Damage Assessment*; ASTM Special Technical Publication: Philadelphia, PA, USA, 1993; Volume 1191, p. 7.
37. You, B.R.; Lee, S.B. A critical review on multiaxial fatigue assessments of metals. *Int. J. Fatigue* **1996**, *18*, 235–244. [[CrossRef](#)]
38. Carpinteri, A.; Brighenti, R.; Spagnoli, A. A fracture plane approach in multiaxial high-cycle fatigue of metals. *Fatigue Fract. Eng. Mater. Struct.* **2000**, *23*, 355–364. [[CrossRef](#)]
39. Karolczuk, A.; Macha, E. A review of critical plane orientations in multiaxial fatigue failure criteria of metallic materials. *Int. J. Fract.* **2005**, *134*, 267–304. [[CrossRef](#)]
40. Marciniak, Z.; Rozumek, D.; Macha, E. Verification of fatigue critical plane position according to variance and damage accumulation methods under multiaxial loading. *Int. J. Fatigue* **2014**, *58*, 84–93. [[CrossRef](#)]
41. Mei, J.; Dong, P. An equivalent stress parameter for multi-axial fatigue evaluation of welded components including non-proportional loading effects. *Int. J. Fatigue* **2017**, *101*, 297–311. [[CrossRef](#)]
42. Farrahi, G.H.; Khalaj, A. Estimation of fatigue damage caused by actual roads and maneuvers on proving ground. *J. Achiev. Mater. Manuf. Eng.* **2006**, *14*, 90–96.
43. Zoroufi, M.; Fatemi, A. Durability comparison and life predictions of competing manufacturing processes: An experimental study of steering knuckle. In Proceedings of the 25th Forging Industry Technical Conference, Detroit, MI, USA, 19–21 April 2004.
44. Fatemi, A.; Zoroufi, M. *Fatigue Performance Evaluation of Forged versus Competing Manufacturing Process Technologies: A Comparative Analytical and Experimental Study*; American Iron and Steel Institute: Washington, DC, USA, 2004.
45. Zoroufi, M.; Fatemi, A. Experimental durability assessment and life prediction of vehicle suspension components: A case study of steering knuckles. *Proc. Inst. Mech. Eng. Part D J. Automob. Eng.* **2006**, *220*, 1565–1579. [[CrossRef](#)]
46. Sonsino, C.M.; Franz, R. Multiaxial fatigue assessment for automotive safety components of cast aluminium EN AC-42000 T6 (G- AlSi7Mg0.3T6) under constant and variable amplitude loading. *Int. J. Fatigue* **2017**, *100*, 489–501. [[CrossRef](#)]
47. d'Ippolito, R.; Hack, M.; Donders, S.; Hermans, L.; Tzannetakis, N.; Vandepitte, D. Improving the fatigue life of a vehicle knuckle with a reliability-based design optimization approach. *J. Stat. Plan. Inference* **2009**, *139*, 1619–1632. [[CrossRef](#)]
48. Ijagbemi, C.O.; Oladapo, B.I.; Campbell, H.M.; Ijagbemi, C.O. Design and simulation of fatigue analysis for a vehicle suspension system (VSS) and its effect on global warming. *Procedia Eng.* **2016**, *159*, 124–132. [[CrossRef](#)]
49. Kulkarni, A.; Ranjha, S.A.; Kapoor, A. Fatigue analysis of a suspension for an in-wheel electric vehicle. *Eng. Fail. Anal.* **2016**, *68*, 150–158. [[CrossRef](#)]
50. Ossa, E.; Palacio, C.; Paniagua, M. Failure analysis of a car suspension system ball joint. *Eng. Fail. Anal.* **2011**, *18*, 1388–1394. [[CrossRef](#)]
51. Kashyzadeh, K.R.; Ostad-Ahmad-Ghorabi, M.J.; Arghavan, A. Fatigue life prediction of package of suspension automotive under random vibration based on road roughness. *Mediterr. J. Model. Simul.* **2015**, *4*, 37–50.

52. Chin, C.H.; Abdullah, S.; Yin, A.G.; Ariffin, A.K. Vibration fatigue analysis through frequency response function of variable amplitude loading. *J. Mech. Sci. Technol.* **2022**, *36*, 33–43. [[CrossRef](#)]
53. Kashyzadeh, K.R.; Farrahi, G.H.; Shariyat, M.; Ahmadian, M.T. Experimental accuracy assessment of various high-cycle fatigue criteria for a critical component with a complicated geometry and multi-input random non-proportional 3D stress components. *Eng. Fail. Anal.* **2018**, *90*, 534–553. [[CrossRef](#)]
54. Kashyzadeh, K.R.; Farrahi, G.H.; Shariyat, M.; Ahmaian, M.T. Experimental and probabilistic approach for assessing fatigue life of automotive steering knuckle. In Proceedings of the 26th Annual International Conference of Iranian Society of Mechanical Engineers—ISME2018, Semnan, Iran, 24–26 April 2018.
55. Kashyzadeh, K.R. A new algorithm for fatigue life assessment of automotive safety components based on the probabilistic approach: The case of the steering knuckle. *Eng. Sci. Technol. Int. J.* **2020**, *23*, 392–404. [[CrossRef](#)]
56. Reza Kashyzadeh, K.; Farrahi, G.H.; Shariyat, M.; Ahmadian, M.T. The Role of Wheel Alignment Over the Fatigue Damage Accumulation in Vehicle Steering Knuckle. *J. Stress Anal.* **2018**, *3*, 21–33. [[CrossRef](#)]
57. Marzbanrad, J.; Hoseinpour, A. Structural optimization of macpherson control arm under fatigue loading. *Teh. Vjesn. Tech. Gaz.* **2017**, *24*, 917–924. [[CrossRef](#)]
58. Farrahi, G.H.; Ahmadi, A.; Kasyzadeh, K.R. Simulation of vehicle body spot weld failures due to fatigue by considering road roughness and vehicle velocity. *Simul. Model. Pract. Theory* **2020**, *105*, 102168. [[CrossRef](#)]
59. Farrahi, G.H.; Ahmadi, A.; Kashyzadeh, K.R.; Azadi, S.; Jahani, K. A comparative study on the fatigue life of the vehicle body spot welds using different numerical techniques: Inertia relief and Modal dynamic analyses. *Frat. Integrità Strutt.* **2020**, *14*, 67–81. [[CrossRef](#)]
60. Taherian, A.H.; Barati, E. A new relation for equalization of load spectrum to a constant amplitude load suitable for fatigue laboratory testing. *Modares Mech. Eng.* **2018**, *17*, 31–38. Available online: <http://dorl.net/dor/20.1001.1.10275940.1396.17.11.32.2> (accessed on 26 March 2022).
61. Pugazhenth, R.; Anbuhezhiyan, G.; Muthuraman, R.K.; Vignesh, M.; Ponshanmugakumar, A. Optimization of fatigue life and fractography analysis of knuckle joint. *Mater. Today Proc.* **2021**, *46*, 4344–4348. [[CrossRef](#)]
62. Reza Kashyzadeh, K.; Ostad-Ahmad-Ghorabi, M.J.; Arghavan, A. Investigating the effect of road roughness on automotive component. *Eng. Fail. Anal.* **2014**, *41*, 96–107. [[CrossRef](#)]
63. Reza Kashyzadeh, K.; Ostad-Ahmad-Ghorabi, M.J.; Arghavan, A. Study effects of vehicle velocity on a road surface roughness simulation. *Appl. Mech. Mater.* **2013**, *372*, 650–656. [[CrossRef](#)]
64. Socie, D.; Marquis, G.B. *Multiaxial Fatigue*; Society of Automotive Engineers: Warrendale, PA, USA, 2000; pp. 129–169.
65. Shariyat, M. A fatigue model developed by modification of Gough's theory, for random non-proportional loading conditions and three-dimensional stress fields. *Int. J. Fatigue* **2008**, *30*, 1248–1258. [[CrossRef](#)]
66. Shariyat, M. Two new multiaxial HCF criteria based on virtual stress amplitude and virtual mean stress concepts for complicated geometries and random nonproportional loading conditions. *J. Eng. Mater. Technol.* **2009**, *131*, 031014. [[CrossRef](#)]
67. Shariyat, M. Three energy-based multiaxial HCF criteria for fatigue life determination in components under random non-proportional stress fields. *Fatigue Fract. Eng. Mater. Struct.* **2009**, *32*, 785–808. [[CrossRef](#)]
68. Carpinteri, A.; Spagnoli, A.; Vantadori, S. Multiaxial fatigue assessment using a simplified critical plane-based criterion. *Int. J. Fatigue* **2011**, *33*, 969–976. [[CrossRef](#)]
69. Carpinteri, A.; Ronchei, C.; Scorza, D.; Vantadori, S. Critical plane orientation influence on multiaxial high-cycle fatigue assessment. *Phys. Mesomech.* **2015**, *18*, 348–354. [[CrossRef](#)]
70. Brod, M.; Dean, A.; Scheffler, S.; Gerendt, C.; Rolfes, R. Numerical modeling and experimental validation of fatigue damage in Cross-Ply CFRP composites under inhomogeneous stress states. *Compos. Part B Eng.* **2020**, *200*, 108050. [[CrossRef](#)]
71. Brod, M.; Just, G.; Dean, A.; Jansen, E.; Koch, I.; Rolfes, R.; Gude, M. Numerical modelling and simulation of fatigue damage in carbon fibre reinforced plastics at different stress ratios. *Thin-Walled Struct.* **2019**, *139*, 219–231. [[CrossRef](#)]
72. Shariyat, M. New multiaxial HCF criteria based on instantaneous fatigue damage tracing in components with complicated geometries and random non-proportional loading conditions. *Int. J. Damage Mech.* **2010**, *19*, 659–690. [[CrossRef](#)]